

Contents lists available at [SciVerse ScienceDirect](http://www.sciencedirect.com)

# Spectrochimica Acta Part A: Molecular and Biomolecular Spectroscopy

journal homepage: [www.elsevier.com/locate/saa](http://www.elsevier.com/locate/saa)

## Synthesis, molecular structure, hydrogen-bonding, NBO and chemical reactivity analysis of a novel 1,9-bis(2-cyano-2-ethoxycarbonylviny)-5-(4-hydroxyphenyl)-dipyrromethane: A combined experimental and theoretical (DFT and QTAIM) approach



R.N. Singh\*, Amit Kumar, R.K. Tiwari, Poonam Rawat

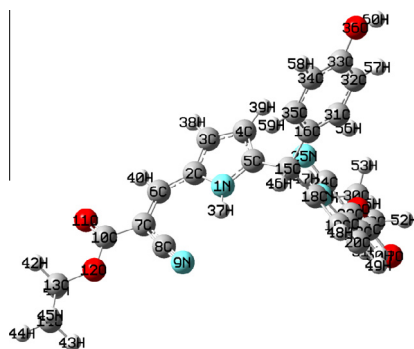
Department of Chemistry, University of Lucknow, Lucknow 226 007, UP, India

### HIGHLIGHTS

- FT-IR spectrum of the studied compound was recorded and compared with the theoretical result.
- All the theoretical calculations were made using DFT/B3LYP/6-31G(d,p) method.
- NBO analysis are performed to determine the hyperconjugative interactions.
- QTAIM analysis are performed to determine hydrogen bonding.
- Chemical reactivity has been explained with the aid of electronic descriptors.

### GRAPHICAL ABSTRACT

A detailed spectroscopic analysis of a newly synthesized 1,9-bis(2-cyano-2-ethoxycarbonylviny)-5-(4-hydroxyphenyl)-dipyrromethane (**3**) have been carried out using  $^1\text{H}$  NMR, UV-Visible, FT-IR and Mass spectroscopic techniques. All the quantum chemical calculations ( $^1\text{H}$  NMR, UV-Visible, FT-IR, NBOs, QTAIM) are carried out using DFT level of theory, B3LYP functional and 6-31G(d,p) as basis set. A combined experimental and theoretical vibrational analysis designates the existence of H-bonding between pyrrole N–H as proton donor and nitrogen of cyanide as proton acceptor. To investigate the strength and nature of H-bonding, topological parameters at bond critical points (BCPs) are analyzed by Bader's 'Quantum theory of Atoms in molecules' in detail. Global electrophilicity index ( $\omega = 4.5281$  eV) shows that title molecule (**3**) is a strong electrophile. Local reactivity descriptors as Fukui functions ( $f_k^+$ ,  $f_k^-$ ), local softnesses ( $s_k^+$ ,  $s_k^-$ ) and electrophilicity indices ( $\omega_k^+$ ,  $\omega_k^-$ ) analyses are performed to find out the reactive sites within molecule.



### ARTICLE INFO

#### Article history:

Received 24 January 2013

Received in revised form 22 April 2013

Accepted 29 April 2013

Available online 15 May 2013

#### Keywords:

Spectroscopic analysis

TD-DFT

### ABSTRACT

The spectroscopic analysis of a newly synthesized 1,9-bis(2-cyano-2-ethoxycarbonylviny)-5-(4-hydroxyphenyl)-dipyrromethane (**3**) has been carried out using  $^1\text{H}$  NMR, UV-Visible, FT-IR and Mass spectroscopic techniques. All the quantum chemical calculations have been carried out using DFT level of theory, B3LYP functional and 6-31G(d,p) as basis set. Thermodynamic parameters ( $H$ ,  $G$ ,  $S$ ) of all the reactants and products have been used to determine the nature of the chemical reaction. The chemical shift of pyrrolic NH in  $^1\text{H}$  NMR spectrum appears at 9.4 ppm due to intramolecular hydrogen bonding. TD-DFT calculation shows the nature of electronic transitions as  $\pi \rightarrow \pi^*$  within the molecule. A combined experimental and theoretical vibrational analysis designates the existence of H-bonding between pyrrole N–H as proton donor and nitrogen of cyanide as proton acceptor, therefore, lowering in stretching

\* Corresponding author. Tel.: +91 9451308205.

E-mail address: [rnsvk.chemistry@gmail.com](mailto:rnsvk.chemistry@gmail.com) (R.N. Singh).

Vibrational analysis  
Hydrogen-bonding  
QTAIM analysis  
Reactivity descriptors

vibration of NH and CN. To investigate the strength and nature of H-bonding, topological parameters at bond critical points (BCPs) are analyzed by 'Quantum theory of Atoms in molecules' (QTAIMs). Natural bond orbitals (NBOs) analysis has been carried out to investigate the intramolecular conjugative and hyperconjugative interactions within molecule and their second order stabilization energy ( $E^{(2)}$ ). Global electrophilicity index ( $\omega = 4.528$  eV) shows that title molecule (**3**) is a strong electrophile. The maximum values of local electrophilic reactivity descriptors ( $f_k^+$ ,  $s_k^+$ ,  $\omega_k^+$ ) at vinyl carbon (C6/C22) of (**3**) indicate that these sites are more prone to nucleophilic attacks.

© 2013 Elsevier B.V. All rights reserved.

## Introduction

Dipyrromethane and its derivatives are the building blocks for the syntheses of a variety of calix[n] pyrroles, porphyrins [1–4], polypyrrolic macrocycles [5], hexaphyrin [6] and corroles [7,8]. The oxidized dipyrromethanes named as dipyrromethenes or dipyrrens give monoanionic, conjugated, planar ligands that have attracted attention in the metal organic framework and have strong coordinating ability towards different metal ions as Li(I), Zn(II), Ni(II), Pd(II/III), Cu(II) and Sn(II) [9–12]. They are reported as versatile ligands for coordination chemistry and supramolecular self-assembly with various transition metal ions [13,14]. The heteroleptic complexes and coordination polymers of dipyrren are used for developing novel magnetic and electronic materials [15–19]. The dipyrrenato metal complexes of Ga(III), In(III) have shown luminescent properties [20] and its several metal-organic frameworks (MOFs) with Ag<sup>+</sup> salts generate strong optical absorption materials [21]. Dipyrromethane based amido-imine hybrid macrocycles have shown oxoanions receptor property [22]. Dipyrrens are also used as ligands for the syntheses of boron dipyrromethene (BODIPY) [23–25], which are used extensively as molecular probes and dyes.

Hydrogen bonds are of versatile importance in fields of chemistry and biochemistry, as they govern chemical reactions, supramolecular structures, molecular assemblies and life processes. Intra and intermolecular hydrogen bonds are classified in two categories depending upon the nature of changes in bond length during the hydrogen bridges formation [26–28].

Cyanovinyl was employed first by Fisher [26,29] as protecting group for formyl in pyrrole for the synthesis of 2,5-diformyl-3,4-dimethylpyrrole and later by Woodward [30] in the synthesis of chlorophyll. The C-vinylpyrrole fragment is found to be reactive for the target synthesis of conjugated and fused heterocycles similar to natural pyrrole assemblies [31,32]. The functionalized C-vinylpyrroles are prospective new materials for molecular optical switches, nanodevices, photo- and electro-conducting applications and also used as ligands for new photo catalysts, biologically active complexes [33–35].

In observation of above applications of cyanovinyl containing dipyrromethane-1,9-bis(2-cyano-2-ethoxycarbonylvinyl)-5-(4-hydroxyphenyl)-dipyrromethane (**3**) has been synthesized and characterized using <sup>1</sup>H NMR, UV-Visible, FT-IR and Mass spectroscopic techniques. Quantum chemical calculations have been carried out using DFT to determine the thermodynamic parameters and the nature of the reaction. The <sup>1</sup>H NMR chemical shifts and vibrational analysis indicated the existence of intramolecular H-bonding. To investigate the strength and nature of intramolecular H-bonding, topological and energetic parameters at bond critical points (BCPs) have been analyzed using QTAIM. NBOs analysis has been carried out to investigate the intramolecular conjugative and hyperconjugative interactions within molecule and their second order stabilization energy. The nature of chemical reactivity and site selectivity of this molecule has been determined on the basis of Global and Local reactivity descriptors [36–41].

## Experimental details

### Synthesis of 1,9-bis(2-cyano-2-ethoxycarbonylvinyl)-5-(4-hydroxyphenyl)-dipyrromethane (**3**)

Ethyl 2-cyano-3-(1H-pyrrol-2-yl)-acrylate (**1**) was prepared by an earlier reported method. To the solution of ethyl 2-cyano-3-(1H-pyrrol-2-yl)-acrylate (0.200 g, 1.0522 mmol) and 4-hydroxybenzaldehyde (0.0642 g, 0.5261 mmol) in 20 ml dichloromethane, p-toluene sulfonic acid (0.0002 g) as catalyst was added. The reaction mixture was refluxed for 8 h, the color of reaction was changed to dark brown and completion of the reaction was analyzed by thin layer chromatography (TLC). Reaction mixture was washed with saturated aqueous solution of NaHCO<sub>3</sub> and extracted with CH<sub>2</sub>Cl<sub>2</sub> (15 ml × 3). The organic layer was dried over MgSO<sub>4</sub> and solvent was removed under reduced pressure. Remaining solid was purified by column chromatography on silica using hexane and ethyl acetate and pure product (**3**) was obtained. Dark brown color compound yielded: 0.1839 g, 72.20%; m.p.: 132–136 °C; DART Mass for C<sub>27</sub>H<sub>24</sub>N<sub>4</sub>O<sub>5</sub>: Calc. 484.1748 amu, Found *m/z* 485.25 [M+H<sup>+</sup>].

## Quantum chemical calculations

All the quantum chemical calculations were carried out with Gaussian 03 program package [42] using B3LYP functional and 6-31G(d,p) basis set [43–45]. Potential energy distribution along internal coordinates was calculated by Gar2ped software. Topological parameters were calculated using software AIM2000 [46].

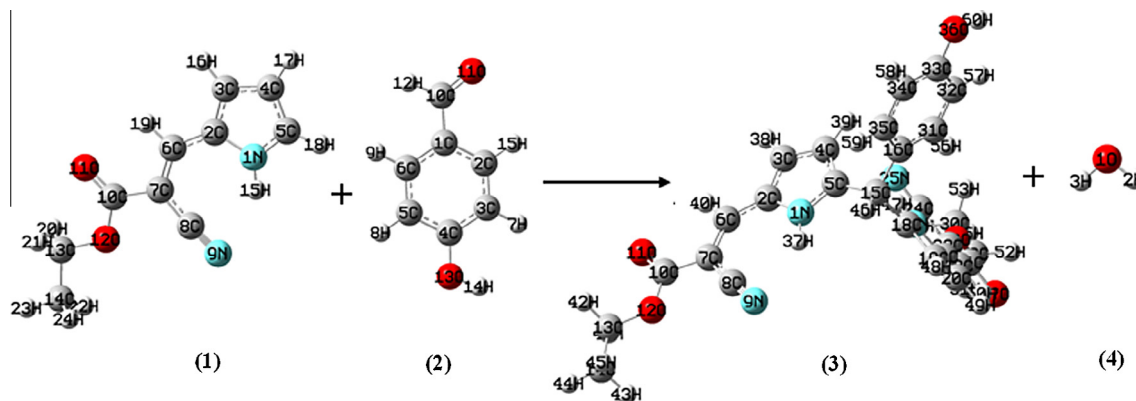
## Results and discussion

### Thermochemistry

Optimized geometry of the reactants ethyl 2-cyano-3-(1H-pyrrol-2-yl)-acrylate (**1**) and 4-hydroxybenzaldehyde (**2**) and product 1,9-bis(2-cyano-2-ethoxycarbonylvinyl)-5-(4-hydroxyphenyl)-dipyrromethane (**3**) and byproduct water (**4**) involved in chemical reaction are shown graphically in Scheme 1. The calculated thermodynamic parameters – Enthalpy (*H*/a.u.), Gibbs free energy (*G*/a.u.) and Entropy [*S*/(cal/mol K)] of (**1**), (**2**), (**3**), (**4**) and their change for Reaction, at 25 °C are listed in Table 1. The calculated negative values of enthalpy change ( $\Delta H$ ) and entropy change ( $\Delta S$ ) show that energy factor is favorable, whereas Gibbs free energy (*G*) factor is unfavorable. The calculated positive value of ( $\Delta G$ ) shows that this reaction is non-spontaneous. At 25 °C, thermodynamic equilibrium constant ( $K_T$ ) for this reaction is calculated as  $2.7883 \times 10^{-7}$  i.e.  $K_{eq} \ll 1$  indicating that the reaction will require elevation of temperature and presence of catalyst.

### Molecular geometry

Optimized geometry for the ground state lower energy conformer of (**3**) is shown in Fig. 1. Selected optimized geometrical parameters of (**3**) are listed in S Table 1 of Supplementary material.



**Scheme 1.** Optimized geometry of reactants (1 and 2), product (3) and byproduct water (4).

**Table 1**

Calculated thermodynamic parameters: Enthalpy ( $H/a.u.$ ), Gibbs free energy ( $G/a.u.$ ) and Entropy [ $S/(cal/mol K)$ ] of (1), (2), (3), (4) and their change for Reaction, at 25 °C.

	(1)	(2)	(3)	(4)	Reaction
$H$	-646.8405	-420.6827	-1637.9773	-76.3945	$\Delta H$ -0.0081
$G$	-646.8971	-420.7230	-1638.0871	-76.4160	$\Delta G$ 0.0142
$S$	119.27	84.71	230.958	45.116	$\Delta S$ -47.176

In (3) two pyrrole units arrange in *anti* form giving the lower energy  $-1638.4802$  a.u. and  $C_1$  symmetry at 25 °C as *anti* forms are reported in the crystal structure of dipyrromethane derivatives [47,48]. The *E*-configuration about the vinyl  $C6=C7$  and  $C22=C23$  bond with respect to the ester and pyrrole give lower energy conformer. The asymmetry in the  $N1-C2$  and  $N1-C5$  bond lengths is explained due to the presence of the two different groups as cyano-vinyl at C2 and substituted methylene group at C5 carbon atom of pyrrole ring.

### $^1H$ NMR spectroscopy

$^1H$  NMR chemical shifts were calculated with GIAO approach [49] and equation:  $\delta_X = IMS_{TMS} - IMS_X$ . The experimental (Fig. 2) and calculated  $^1H$  NMR chemical shifts ( $\delta$ , ppm) with assignment for (3) are given in Table 2. In order to compare the chemical shifts, correlation graphs between the experimental and calculated  $^1H$  NMR chemical shifts are shown in S Fig. 1 of Supplementary material. The correlation coefficients ( $R^2 = 0.97284$ ) shows that there is good agreement between experimental and calculated chemical shifts.

### UV-Visible spectroscopy

The nature of the transitions in UV-Visible spectrum of the title compound has been studied by TD-DFT. The comparison between experimental and theoretical UV-Visible spectra for (3) is shown in Fig. 3. The experimental and calculated electronic transitions parameters are listed in Table 3. TD-DFT calculations predict two electronic transitions at 217 nm and 345 nm which correspond to the experimental electronic transitions observed at 214, 304 nm, respectively. S Fig. 2 of Supplementary material shows that the orbitals H-1 and H are localized over  $C34-C35$  and  $C16-C31$  of benzene ring, whereas orbitals L+1 and L+6 are localized over  $C10-O11$  of carbonyl in ester and  $C22-C23$  vinyl bond, respectively. On the basis of molecular orbital coefficients analysis and molecular orbital plots, the nature of these electronic excitations are assigned to be  $\pi(C16-C31) \rightarrow \pi^*(C22-C23)$ ,  $\pi(C34-C35) \rightarrow \pi^*(C10-O11)$ , respectively.

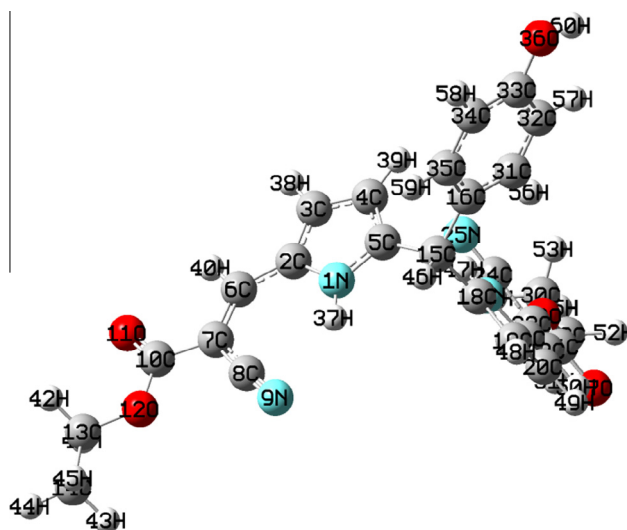


**Fig. 1.** Optimized geometry for the ground state lower energy conformer of (3).

**Table 2**

Experimental and calculated  $^1H$  NMR chemical shifts ( $\delta$ , ppm) in MeOD as the solvent at 25 °C for (3) with assignment.

Atom No.	$\delta_{calcd}$	$\delta_{exp}$	Assignment
H37	9.9008	9.4014	s, 2 × 1H, pyrrole-NH
H38	6.9441	6.6567–6.6749	d, 2 × 1H, pyrrole-CH
H39	6.1525	6.3382–6.3569	d, 2 × 1H, pyrrole-CH
H40	7.8738	7.8908	s, 2 × 1H, vinyl-CH
H41	4.2458	4.3167–4.3878	q, $J = 7.11$ Hz, 2 × 2H, ester-CH <sub>2</sub>
H42	4.2628		
H43	1.4291	1.3640–1.4115	t, $J = 7.125$ Hz, 2 × 3H, ester-CH <sub>3</sub>
H44	1.2191		
H45	1.4365		
H46	5.4448	5.1904	s, 1H, meso-CH
H47	9.6731	9.4014	s, 2 × 1H, pyrrole-NH
H48	6.4576	6.6749–6.6567	
H49	7.0167	6.3382–6.3569	
H50	7.8247	7.8908	s, 2 × 1H, vinyl-CH
H51	4.2331	4.3167–4.3878	q, $J = 7.11$ Hz, 2 × 2H, ester-CH <sub>2</sub>
H52	4.2525		
H53	1.4294	1.3640–1.4115	t, $J = 7.125$ Hz, 2 × 3H, ester-CH <sub>3</sub>
H54	1.4136		
H55	1.2122		
H56	7.1541	7.1567–7.4212	m, 4H, benzene ring
H57	6.724		
H58	6.9478		
H59	7.3625		
H60	4.409	5.6308	s, 1H, -OH

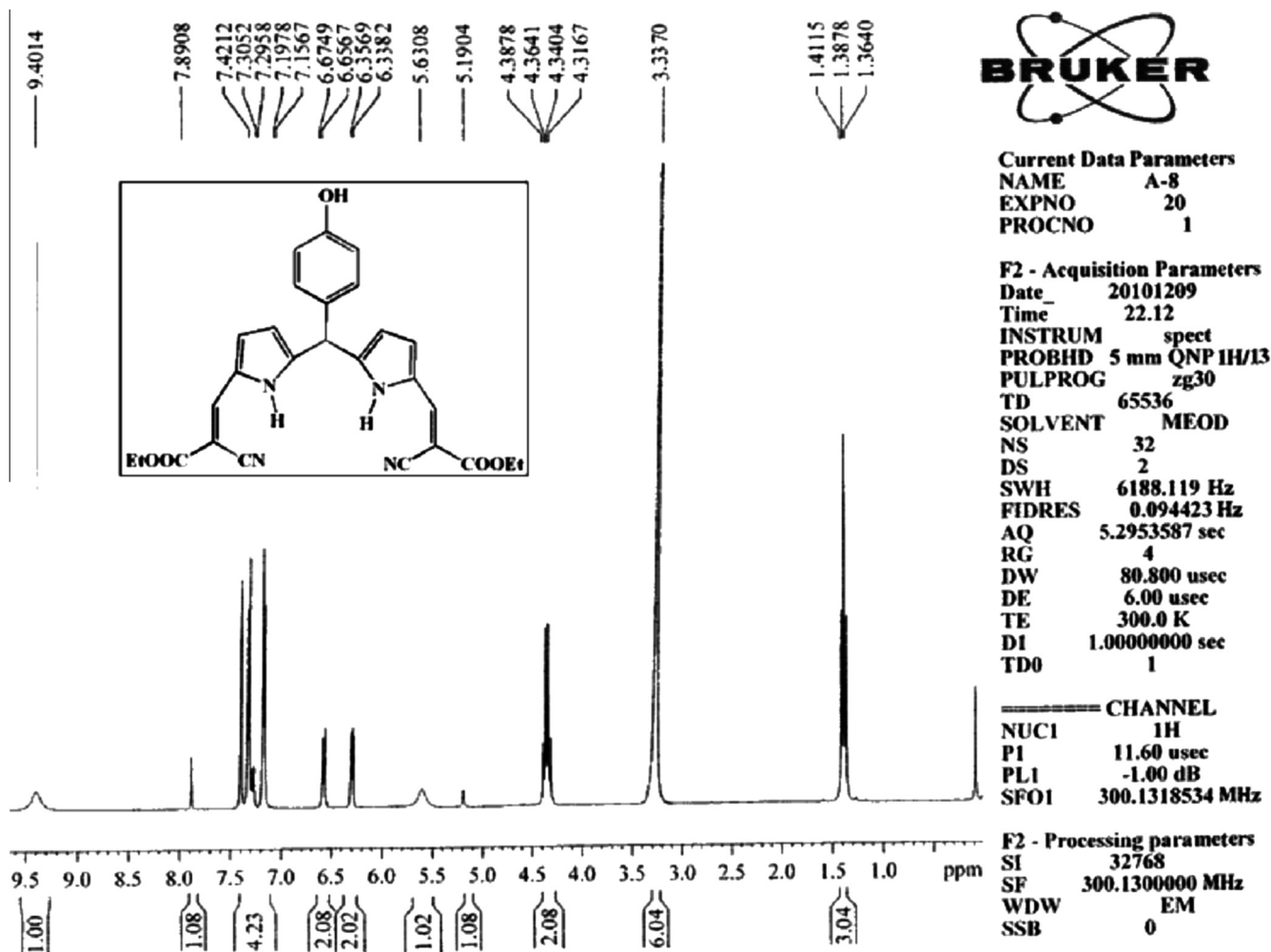


Fig. 2. The experimental  $^1\text{H}$  NMR spectrum of (3) in MeOD solvent.

#### Natural bond orbitals (NBOs) analysis

The strength of various types of interactions or stabilization energy ( $E^{(2)}$ ) associated with electron delocalization between each donor NBO( $i$ ) and acceptor NBO( $j$ ) is estimated by the second order energy lowering equation [50–53]. Second-order perturbation theory analysis of the Fock matrix in NBO basis for (3) is presented in S Table 2 of Supplementary material. The interactions  $\pi(\text{C}2-\text{C}3) \rightarrow \pi^*(\text{C}4-\text{C}5)$  and  $\pi(\text{C}4-\text{C}5) \rightarrow \pi^*(\text{C}2-\text{C}3)$  are responsible for the conjugation of respective  $\pi$ -bonds in pyrrole ring. The electron density at the conjugated  $\pi$  bonds (1.688–1.722) and  $\pi^*$  bonds (0.369–0.420) of pyrrole ring indicate strong  $\pi$ -electron delocalization within ring leading to a maximum stabilization of energy up to  $\sim 22.99$  kcal/mol. The interaction  $n_1(\text{N}1) \rightarrow \pi^*(\text{C}2-\text{C}3)/\pi^*(\text{C}4-\text{C}5)$  indicate the involvement of lone-pair of pyrrole N atom with  $\pi$ -electron delocalization in ring. The interactions  $\pi(\text{C}2-\text{C}3) \rightarrow \pi^*(\text{C}6-\text{C}7)$ ,  $\pi(\text{C}6-\text{C}7) \rightarrow \pi^*(\text{C}2-\text{C}3)$  are responsible for the conjugation of bonds C2–C3 and C6–C7 with C2–C6 and stabilized the molecule up to  $\sim 27.34$  kcal/mol. The electron density at the conjugated  $\pi$  bonds (1.653–1.702) and  $\pi^*$  bonds (0.321–0.387) of benzene ring indicate strong  $\pi$ -electron delocalization within ring leading to a maximum stabilization of energy up to  $\sim 22.51$  kcal/mol.

The primary hyperconjugative interactions  $n_1(\text{N}9) \rightarrow \sigma^*(\text{C}7-\text{C}8)$  and  $n_2(\text{O}11) \rightarrow \sigma^*(\text{C}10-\text{O}12)$  stabilize the molecule by 32.63 kcal/mol. The secondary hyperconjugative interactions asso-

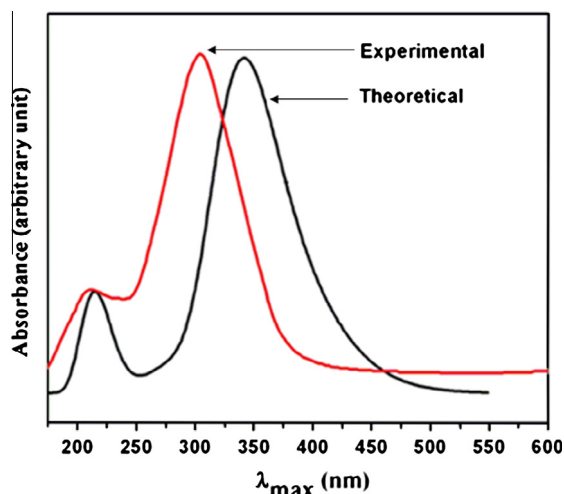


Fig. 3. Comparison between experimental and theoretical UV-Visible spectra for (3).

ciated with the pyrrole ring such as  $\sigma(\text{N}1-\text{C}2) \rightarrow \sigma^*(\text{C}5-\text{C}15)$ ,  $\sigma(\text{N}1-\text{C}5) \rightarrow \sigma^*(\text{C}2-\text{C}6)$ ,  $\sigma(\text{C}2-\text{C}3) \rightarrow \sigma^*(\text{C}2-\text{C}6)$ ,  $\sigma(\text{C}3-\text{C}4) \rightarrow \sigma^*(\text{C}2-\text{C}6)$  and  $\sigma(\text{C}4-\text{C}5) \rightarrow \sigma^*(\text{N}1-\text{H}37)$  stabilize the molecule within range 3.26–5.42 kcal/mol.

**Table 3**Experimental and calculated electronic transitions for (**3**):  $E/eV$ , oscillatory strength ( $f$ ), ( $\lambda_{\max}/nm$ ) at TD-DFT/B3LYP/6-31G(d,p) level.

S. no.	Excitations	$E$ (eV)	$f$	$\lambda_{\max}$ calcd.	$\lambda_{\max}$ obs.	Assignment
1	H-1 → L+1	3.5914	0.7157	345.22	304	$\pi(C34-C35) \rightarrow \pi^*(C10-O11)$
2	H → L+6	5.7059	0.0441	217.29	214	$\pi(C16-C31) \rightarrow \pi^*(C22-C23)$

Selected Lewis orbitals (occupied bond or lone pair) of (**3**) with their valence hybrids are listed in S Table 3 of Supplementary material. The valence hybrids analysis of NBO orbitals shows that all the N–H/C–N and C–O bond orbitals are polarized towards the nitrogen (ED = 57.50–73.94% at N), oxygen (ED = 65.52–68.78% at O), respectively. The electron density distribution (occupancy) around the lone pair of O and N atoms mainly influences the polarity of the compound.

### Vibrational assignments

The experimental and theoretical (selected) vibrational wavenumbers of (**3**), calculated at B3LYP/6-31G(d,p) method and their assignments using PED are given in Table 4. The total number of atoms ( $n$ ) in monomer (**3**) is 60, therefore this gives 174,  $(3n-6)$  vibrational modes. Calculated wavenumbers were scaled down using scaling factor 0.9608 [54], to discard the anharmonicity pres-

**Table 4**Experimental and theoretical [calculated at B3LYP/6-31G(d,p) level] vibrational wavenumbers of (**3**) and their assignments: Wavenumbers ( $\bar{\nu}/cm^{-1}$ ), intensity ( $K\text{ mmol}^{-1}$ ).

$\bar{\nu}$ unscal.	$\bar{\nu}$ scaled	$IR_{\text{int}}$	$\bar{\nu}$ Exp.	Assignment (PED) $\geq 5\%$
3821	3671	61.25	3409	$\nu(O36H60)(100)$
3598	3456	88.13	3336	$\nu(N1H37)(99)$
3 584	3443	77.18		$\nu(N17H47)(99)$
3170	3045	22.35	3036	$\nu(C32H57)(93)-\nu(C31H56)(5)$
3133	3010	24.65	2980	$\nu(C14H44)(58)-\nu(C14H45)(19)-\nu(C14H43)(17)$
3133	3010	26.69		$\nu(C30H55)(59)-\nu(C30H53)(19)-\nu(C30H54)(17)$
3066	2945	20.99	2928	$\nu(C13H41)(49)+\nu(C13H42)(49)$
3066	2945	22.65		$\nu(C29H52)(50)+\nu(C29H51)(48)$
2311	2220	43.67	2213	$\nu(C24N25)(86)-\nu(C23C24)(13)$
2310	2219	40.76		$\nu(C8N9)(87)-\nu(C7C8)(12)$
1794	1723	212.24		$\nu(C10011)(76)-\nu(C10012)(6)-(\delta ip-C7C10)(5)$
1793	1722	275.48	1701	$\nu(C26O27)(76)-(\delta-C23C26)(6)-\nu(C26O28)(6)$
1672	1606	56.28		$\nu(C34C35)(20)+\nu(C31C32)(19)-\nu(C33C34)(11)+(\delta as-R1)(11)-\nu(C16C31)(9)+(\delta-C16H56C31)(6)$
1647	1582	290.59		$\nu(C6C7)(14)-\nu(C2C6)(13)+\nu(C22C23)(9)-\nu(C21C22)(8)-\nu(C32C33)(6)-(\delta ip-C2C6)(5)+\nu(C2C3)(5)$
1645	1580	580.65	1587	$\nu(C22C23)(18)-\nu(C21C22)(17)-\nu(C6C7)(10)+\nu(C2C6)(10)-(\delta ip-C21C22)(6)+\nu(C20C21)(6)$
1643	1578	251.49		$\nu(C32C33)(17)+\nu(C16C35)(13)-\nu(C33C34)(11)-\nu(C16C31)(7)+(\delta as-R1)(6)+\nu(C6C7)(5)$
1586	1523	191		$\nu(C6C7)(19)+(\delta-C2H37N1)(16)+\nu(C4H39)(12)$
1582	1519	346.64	1483	$\nu(C22C23)(19)-(\delta-C18H47N17)(13)+\nu(C18C19)(11)-\nu(C6C7)(7)-\nu(C15C18)(6)$
1559	1497	148.62	1453	$(\delta-C34H59C35)(14)-(\delta-C31H57C32)(13)-(\delta-C16H56C31)(13)+\nu(C16C31)(11)+\nu(C33O36)(9)-\nu(C33C34)(9)-\nu(C32C33)(8)-(\delta-C35H58C34)(8)$
1532	1471	7.3		$(\delta sc-CH2)(41)-(\delta sc-CH2)(24)-(\delta as-Me)(11)+(\delta as-Me)(8)+(\delta as-Me)(3)+(\delta sc-C13C14O12)(2)-(\rho-Me)(2)$
1499	1440	5.19		$(\delta as-Me)(67)+(\delta as-Me)(24)-(\rho-Me)(6)$
1520	1460	46.52		$\nu(C3C4)(13)-\nu(N1C5)(12)-\nu(C2C3)(7)-(\delta-R)(7)+\nu(C5C15)(6)-\nu(C19C20)(6)+\nu(N17C18)(5)$
1438	1381	25.36	1368	$\nu(N17C21)(24)-\nu(C20C21)(18)+(\delta s-Me)(12)+(\delta-C18H47N17)(7)-(\delta-C18H48C19)(6)-(\delta-R)(5)-(\delta-N17C22C21)(5)$
1405	1349	20		$(\omega-CH2)(46)-(\delta s-Me)(31)$
1405	1349	21.08	1344	$(\omega-CH2)(45)-(\delta s-Me)(32)$
1351	1298	39.69	1253	$(\delta ip-C2C6)(28)+\nu(C3C4)(17)+\nu(C7C10)(7)-(\delta-C3H39C4)(7)+(\delta-C2H37N1)(5)-\nu(C7C8)(5)$
1299	1248	0.71		$(t-CH2)(86)-(\rho-Me)(8)$
1289	1238	568.13		$\nu(C26O28)(16)+(\delta-C18H47N17)(11)-\nu(C23C26)(9)-\nu(C15C18)(8)+(\delta ip-O27C26O28)(5)+(\omega-CH2)(5)$
1285	1234	898.49		$\nu(C10012)(22)-\nu(C7C10)(16)-(\delta-O11O12C10)(8)+(\omega-CH2)(7)$
1199	1151	579.88	1094	$(\delta-C3H39C4)(9)+(\rho-C15H46)(9)+(\delta-C2H37N1)(8)+(\delta-C2H38C3)(8)-\nu(N1C5)(7)+\nu(C10012)(7)+\nu(C5C15)(6)-\nu(C2C6)(5)+\nu(C2C3)(5)$
1145	1100	0.84		$(\rho-Me)(16)-\nu(C13C14)(12)+(\delta sc-C13C14O12)(9)-(\rho-Me)(6)-\nu(C10012)(6)-\nu(C29C30)(5)-(\rho-Me)(5)$
1129	1084	60.84	1047	$\nu(O12C13)(12)+\nu(O28C29)(8)+\nu(C7C8)(7)-(\rho-Me)(7)-\nu(C7C10)(6)-(\delta-C22C23C24)(5)+(\delta ip-C2C6)(5)-\nu(C10012)(5)+\nu(C23C24)(5)$
1129	1084	97.75	1047	$\nu(O28C29)(12)-(\delta-C22C23C24)(8)+\nu(C23C24)(7)-\nu(O12C13)(7)+(\rho-Me)(6)-\nu(C23C26)(6)-\nu(C26O28)(5)+(\delta ip-C21C22)(5)$
1078	1035	111.84	1018	$(\delta-C18H48C19)(35)-(\delta-C19H49C20)(30)-\nu(C19C20)(24)$
1075	1032	86.93		$(\delta-C3H39C4)(35)-(\delta-C2H38C3)(30)+\nu(C3C4)(24)$
1050	1008	47.82	994	$\nu(C13C14)(26)-\nu(O12C13)(22)-\nu(C29C30)(11)+\nu(O28C29)(9)$
1049	1007	41.95		$\nu(C29C30)(27)-\nu(O28C29)(22)+\nu(C13C14)(11)-\nu(O12C13)(9)$
906	870	21.62	879	$\nu(O12C13)(16)-\nu(O28C29)(15)+(\rho-Me)(8)+\nu(C13C14)(8)-\nu(C29C30)(7)+(\rho-Me)(6)$
906	870	12.94		$\nu(O28C29)(17)+\nu(O12C13)(14)+\nu(C29C30)(8)+(\rho-Me)(7)-(\rho-Me)(7)+\nu(C13C14)(7)$
800	768	55.96	757	$(\omega-C4H39)(34)+(\omega-C3H38)(25)+(\delta-R)(9)+(\delta-C23C22C21)(5)$
798	766	35.11		$(\omega-C19H48)(33)+(\omega-C20H49)(19)$
711	683	44.46	663	$(\tau-R)(27)-(\tau-R1-Puckering)(10)+(\delta oop-C15C18)(9)-(\tau-C21C22)(5)$
697	669	41.22		$(R1-Puckering)(33)+(\tau-R)(8)+(\delta oop-C33O36)(7)+(\delta-R)(6)$
636	611	15.51		$(\omega-N17H47)(28)+(\tau-R)(12)+(\delta as-R1)(10)+(\omega-N1H37)(7)$

Proposed assignment and potential energy distribution (PED) for vibrational modes: Types of vibrations:  $\nu$  – stretching,  $\rho$  – rocking,  $\omega$  – wagging,  $\delta$  – deformation,  $\delta s$  – symmetric deformation,  $\delta as$  – asymmetric deformation,  $\delta ip$  – in plane deformation,  $\delta oop$  – out-of-plane deformation,  $\tau$  – torsion. R – pyrrole ring, R1 – benzene ring, Me – ester methyl.

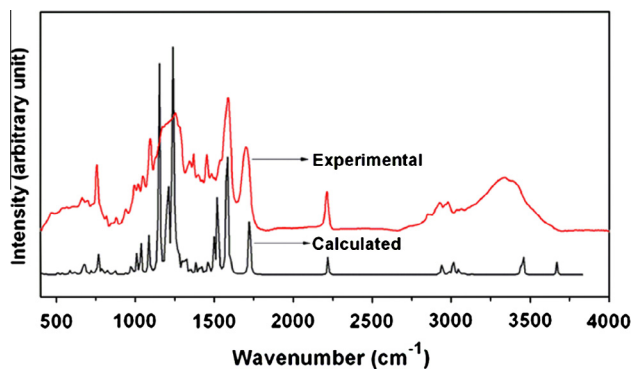


Fig. 4. Comparison between experimental and theoretical IR spectra for (3).

ent in real system. Comparison among experimental and theoretical (selected) IR spectra for (3) in the region 4000–400  $\text{cm}^{-1}$  is shown in Fig. 4.

#### N–H and O–H vibrations

In the FT-IR spectrum of (3), the N–H stretch of pyrrole ( $\nu_{\text{N-H}}$ ) is observed at 3336  $\text{cm}^{-1}$ , whereas this is calculated at 3456  $\text{cm}^{-1}$  in one pyrrole unit and at 3443  $\text{cm}^{-1}$  in other pyrrole unit of the investigated molecule. The observed  $\nu_{\text{N-H}}$  for pyrrole at 3336 is in good agreement with the earlier reported hydrogen bonded  $\nu_{\text{N-H}}$  at 3358  $\text{cm}^{-1}$  recorded in KBr pellet, but it deviates from the reported free  $\nu_{\text{NH}}$  band observed at higher wavenumber 3465  $\text{cm}^{-1}$ , recorded in  $\text{CCl}_4$  solution [55]. The observed  $\nu_{\text{N-H}}$  for pyrrole also deviates from the free  $\nu_{\text{N-H}}$  of pyrrole at 3475  $\text{cm}^{-1}$ , reported in literature [56]. Therefore, the red shift in the observed  $\nu_{\text{N-H}}$  of pyrrole compared with free  $\nu_{\text{N-H}}$  indicates the involvement of the N–H group in intramolecular hydrogen bonding. The calculated wavenumbers at 611  $\text{cm}^{-1}$  is assigned to the wagging mode of pyrrole (N–H) and matches well with the observed wavenumber at 608  $\text{cm}^{-1}$ . The calculated wavenumber at 3671  $\text{cm}^{-1}$  demonstrates the presence of O–H stretch of phenol ( $\nu_{\text{O-H}}$ ) and observed about 3409  $\text{cm}^{-1}$  in the experimental FT-IR spectrum. It is to be noticed that N–H and O–H stretches are merged to each other due to broadening of the peak.

#### C–H vibrations

Two ester methyl (Me) and two ester  $\text{CH}_2$  groups are present in the investigated molecule (3). The theoretical vibrational analysis displays the presence of asymmetric C–H stretching vibrations of ester methyl group at 3010  $\text{cm}^{-1}$  and it is observed at 2980  $\text{cm}^{-1}$  in the experimental FT-IR spectrum. These observed vibrations of the methyl groups also correspond to the reported absorption bands in the literature such as asymmetric stretches at  $2985 \pm 25 \text{ cm}^{-1}$ , and symmetric stretches at  $2920 \pm 80 \text{ cm}^{-1}$  [57]. The asymmetric and symmetric deformation modes of Me are assigned at 1440, 1349  $\text{cm}^{-1}$ , respectively. The symmetric deformation mode of Me assigned at 1349  $\text{cm}^{-1}$  matches well with the observed wavenumber at 1344  $\text{cm}^{-1}$ . The rocking mode of Me group calculated at 1084  $\text{cm}^{-1}$  with 7% contribution in PED corresponds to the observed wavenumber at 1047  $\text{cm}^{-1}$ . According to Internal coordinate system recommended by Pulay et al. [58],  $\text{CH}_2$  group associate with six types of vibrational frequencies namely: symmetric stretch, asymmetric stretch, scissoring, rocking, wagging and twisting. The scissoring and rocking deformations belong to polarized in-plane vibration, whereas wagging and twisting deformations belong to depolarized out-of-plane vibration. The theoretical vibrational analysis indicates the presence of C–H stretching vibration of ester  $\text{CH}_2$  group at 2945  $\text{cm}^{-1}$  and corresponds to the observed wavenumber at 2928  $\text{cm}^{-1}$  in the experi-

mental FT-IR spectrum. These observed vibrations of the  $\text{CH}_2$  groups are also correspond to the reported absorption bands in the literature such as asymmetric stretches at  $3000 \pm 50 \text{ cm}^{-1}$ , and symmetric stretches at  $2965 \pm 30 \text{ cm}^{-1}$  [57]. The calculated wavenumber 1471  $\text{cm}^{-1}$  is assigned to the scissoring mode of  $\text{CH}_2$  group. The calculated wavenumber at 1349  $\text{cm}^{-1}$  describes the presence of wagging mode of  $\text{CH}_2$  group and agrees well with the observed wavenumber at 1344  $\text{cm}^{-1}$ . These observed deformation modes of the  $\text{CH}_2$  groups are also correspond to the reported absorption bands in the literature for scissoring modes at  $1455 \pm 55 \text{ cm}^{-1}$  and wagging modes at  $1350 \pm 85 \text{ cm}^{-1}$ . The calculated C–H stretching vibration of benzene at 3045  $\text{cm}^{-1}$  matches well with the observed wavenumber at 3036  $\text{cm}^{-1}$ . The calculated wavenumber at 683  $\text{cm}^{-1}$  is assigned to the puckering vibration (a torsional mode) of benzene ring and observed at 663  $\text{cm}^{-1}$  in the experimental FT-IR spectrum.

#### C=O, C–O vibrations

The investigated molecule (3) contains two carbonyl groups ( $\text{C}10=\text{O}11$ ,  $\text{C}26=\text{O}27$ ) and two vinyl groups ( $\text{C}6=\text{C}7$ ,  $\text{C}22=\text{C}23$ ) due to the symmetrical nature of molecule. The stretching vibration of ester carbonyl group ( $\nu_{\text{C=O}}$ ) is observed at 1701  $\text{cm}^{-1}$ , whereas this is calculated at 1722  $\text{cm}^{-1}$  in theoretical IR-spectrum. The “C–O stretching vibrations” of esters actually consists of two asymmetrical coupled vibrations as  $\text{O}-\text{C}(=\text{O})-\text{C}$  and  $\text{O}-\text{C}-\text{C}$  and these bands occur in the region 1300–1000  $\text{cm}^{-1}$  [59]. The ester  $\text{O}-\text{C}(=\text{O})-\text{C}$  stretching vibration as  $\nu_{\text{C}26-\text{O}28}$  is assigned at 1238  $\text{cm}^{-1}$ . The calculated wavenumber at 1234  $\text{cm}^{-1}$  is assigned to a combination band of ester stretching  $\nu_{\text{C}10-\text{O}12}$  and its deformation  $\text{O}11-\text{O}12-\text{C}10$  with 8% contribution in PED. The calculated wavenumber at 1084  $\text{cm}^{-1}$  is demonstrated to the  $\text{O}-\text{C}-\text{C}$  stretching vibration of ester groups as  $\nu_{\text{O}12-\text{C}13}$ ,  $\nu_{\text{O}28-\text{C}29}$  and corresponds to the observed wavenumber at 1047  $\text{cm}^{-1}$  in the experimental FT-IR spectrum.

#### C–C vibrations

The C=C stretches in benzene ring are assigned at 1606, 1578  $\text{cm}^{-1}$  and correspond to the observed band reported in literature in the region 1600–1585  $\text{cm}^{-1}$  [59]. The calculated wavenumbers at 1580, 1519  $\text{cm}^{-1}$  exhibit presence of the C=C stretches of vinyl groups ( $\nu_{\text{C}22=\text{C}23}$ ,  $\nu_{\text{C}6=\text{C}7}$ ) and observed at 1587, 1483  $\text{cm}^{-1}$ , respectively in the experimental FT-IR spectrum. An observed combination band of ‘pyrrole ring stretches and its deformations’ at 1368  $\text{cm}^{-1}$  corresponds with the calculated wavenumber at 1381  $\text{cm}^{-1}$ . The calculated wavenumber at 1460  $\text{cm}^{-1}$  also describes the presence of the C–C stretch of pyrrole up to 13% contribution in PED. The deformation modes associated with pyrrole ring are calculated at 1298, 1151, 1035  $\text{cm}^{-1}$ , whereas these are observed at 1253, 1094, 1018  $\text{cm}^{-1}$ , respectively. The calculated wavenumber at 768  $\text{cm}^{-1}$  is assigned to the C–H wagging mode of pyrrole and matches with the observed wavenumber at 757  $\text{cm}^{-1}$ . The C–C stretches of ester calculated at 1008  $\text{cm}^{-1}$  corresponds to the observed wavenumber at 994  $\text{cm}^{-1}$ .

#### C≡N vibrations

In the theoretical IR spectrum of (3), the calculated wavenumber at 2220  $\text{cm}^{-1}$  designates the presence of the C≡N stretching vibration and agrees well with the observed wavenumber at 2213  $\text{cm}^{-1}$ . The free C≡N stretching vibrations are reported in literature in the region 2240–2260  $\text{cm}^{-1}$  [56]. Therefore, the red shift in the observed C≡N stretching compared with the free C≡N stretching indicates the involvement of the C≡N group in intramolecular hydrogen bonding.

### Quantum Theory of Atoms in Molecules (QTAIMs) analysis

Molecular graph of (**3**) using QTAIM program at B3LYP/6-31G(d,p) level is shown in S Fig. 2 of Supplementary material. Topological as well as geometrical parameters for bonds of interacting atoms are given in S Tables 4 and 5 of Supplementary material, respectively. The nature of interactions indicated in the molecular graph depends upon the geometrical, topological and energetic parameters. For intramolecular interactions (N1—H37...N9, N17—H47...N25), the electron density ( $\rho_{\text{H}1\cdots\text{A}}$ ) and its Laplacian ( $\nabla^2_{\rho_{\text{BCP}}}$ ) are in the range 0.0133–0.0143, 0.0470–0.0498 a.u., respectively. Therefore, these interactions follow the Koch and Popelier criteria [60]. The nature of these interactions (intramolecular classical hydrogen bonds) is weak as ( $\nabla^2_{\rho_{\text{BCP}}}$ ) > 0 and  $H_{\text{BCP}} > 0$  at bond critical point. The energy of intramolecular [61,62] classical hydrogen bonds N1—H37...N9 and N17—H47...N25 are calculated to be –2.76, –2.54 kcal/mol, respectively.

### Chemical reactivity

#### Global reactivity descriptors

Global reactivity descriptors [37–41] electronegativity ( $\chi$ ) =  $-1/2 (\epsilon_{\text{LUMO}} + \epsilon_{\text{HOMO}})$ , chemical potential ( $\mu$ ) =  $1/2 (\epsilon_{\text{LUMO}} + \epsilon_{\text{HOMO}})$ , global hardness ( $\eta$ ) =  $1/2 (\epsilon_{\text{LUMO}} - \epsilon_{\text{HOMO}})$ , global softness ( $S$ ) =  $1/2\eta$  and electrophilicity index ( $\omega$ ) =  $\mu^2/2\eta$ , determined on the basis of Koopman's theorem [36] for (**1**), (**2**), (**3**) and ECT =  $(\Delta N_{\text{max}})_A - (\Delta N_{\text{max}})_B$  [63] for reactant system [(**1**) ↔ (**2**)] are listed in S Table 6 of Supplementary material. The global electrophilicity index ( $\omega$ ) = 4.53 eV of (**3**) shows it as a strong electrophile. ECT calculated as 0.54264 for reactant system [(**1**) ↔ (**2**)], indicates that charge flows from (**2**) to (**1**).

#### Local reactivity descriptors

Selected nucleophilic reactivity descriptors ( $f_{\text{k}}^-, s_{\text{k}}^-, \omega_{\text{k}}^-$ ) [37–41] for reactant (**1**), using Mulliken atomic charges are given in S Table 7 of Supplementary material. In reactant (**1**), the maximum values of the local nucleophilic reactivity descriptors ( $f_{\text{k}}^-, s_{\text{k}}^-, \omega_{\text{k}}^-$ ) at C5 indicate that this site is prone to electrophilic attack. It is to be noticed that the reactants (**2**), possess only one carbonyl functional group (>C=O), therefore for (**2**) there is no need to calculate the local electrophilic reactivity descriptors ( $f_{\text{k}}^+, s_{\text{k}}^+, \omega_{\text{k}}^+$ ). Thus, Local reactivity descriptors for reactant (**1**) confirm the formation of product (**3**) by nucleophilic attack of the C5 carbon atom of (**1**) on the more electrophilic carbonyl carbon (C11) of the reactant (**2**). Selected electrophilic reactivity descriptors ( $f_{\text{k}}^+, s_{\text{k}}^+, \omega_{\text{k}}^+$ ) for (**3**), using Mulliken atomic charges are given in S Table 8 of Supplementary material. The maximum values of local electrophilic reactivity descriptors ( $f_{\text{k}}^+, s_{\text{k}}^+, \omega_{\text{k}}^+$ ) at vinyl carbons (C6/C22) of (**3**) indicate that these sites are more prone to nucleophilic attack and favor the formation of the unsymmetrical dipyrromethane.

### Conclusions

The title compound (**3**) has been synthesized and characterized by experimental and theoretical techniques. The calculated  $^1\text{H}$  NMR chemical shifts are in agreement with the experimentally observed chemical shifts. The TD-DFT/B3LYP calculations show that observed wavelength absorption maxima ( $\lambda_{\text{max}}$ ) have some blue shifts compared with the calculated  $\lambda_{\text{max}}$ . A combined molecular orbital coefficients analysis and molecular orbital plots suggests that the nature of electronic excitations is  $\pi \rightarrow \pi^*$ . NBOs analysis exhibits various types of intramolecular conjugative and hyperconjugative interactions being responsible for  $\pi$ -electron delocalization within pyrrole and benzene rings and stabilizes the molecule with energy in the region from 3.19 to 44.04 kcal/mol.

A combined experimental and theoretical vibrational analysis designates the existence of intramolecular classical hydrogen bonds (N1—H37...N9 and N17—H47...N25) between pyrrole N—H as proton donor and cyanide as proton acceptor. QTAIM calculated topological, geometrical and energetic parameters indicate the nature of intramolecular classical hydrogen bonds as weak with energy values –2.54 to –2.76 kcal/mol. The global electrophilicity index ( $\omega$ ) = 4.5281 eV of (**3**) indicates its behavior as a strong electrophile. The electrophilic reactivity descriptors analyses of (**3**) indicate that the investigated molecule might be used as precursor for the target syntheses of unsymmetrical dipyrromethane derivatives.

### Acknowledgment

The authors are thankful to the CSIR for financial support.

### Appendix A. Supplementary Material

Supplementary data associated with this article can be found, in the online version, at <http://dx.doi.org/10.1016/j.saa.2013.04.121>.

### References

- [1] J.S. Lindsey, Metalloporphyrins Catalysed Oxidation, Kluwer Academic Publishers, The Netherlands, 1994.
- [2] S.-J. Hong, M.-H. Lee, C.-H. Lee, Bull. Korean Chem. Soc. 25 (2004) 1545–1550.
- [3] W.-S. Cho, H.-Je Kim, B.J. Littler, M.A. Miller, C.-H. Lee, J.S. Lindsey, J. Org. Chem. 64 (1999) 7890–7901.
- [4] R.L. Halterman, X. Mei, Tetrahedron Lett. 37 (1996) 6291–6294.
- [5] A. Jasat, D. Dolphin, Chem. Rev. (1997) 2277–2282.
- [6] G. Mori, H. Shinokubo, A. Osuka, Tetrahedron Lett. 49 (2008) 2170–2172.
- [7] R. Guillard, D.T. Gryko, G. Canard, J.-M. Barbe, B. Koszarna, S. Brande's, M. Tasior, Org. Lett. 4 (2002) 4491–4494.
- [8] M. Schwalbe, D.K. Dogutan, S.A. Stojan, T.S. Teets, D.G. Nocera, Inorg. Chem. 50 (2011) 1368–1377.
- [9] J.C. Wechsler, A.A.-S. Ali, E.E. Chapman, T.S. Cameron, A. Thompson, Inorg. Chem. 46 (2007) 10947–10949.
- [10] L. Yu, K. Muthukumar, I.V. Sazanovich, C. Kirmaier, E. Hindin, J.R. Diers, P.D. Boyle, D.F. Bocian, D. Holten, J.S. Lindsey, Inorg. Chem. 42 (2003) 6629–6647.
- [11] C. Brückner, V. Karunaratne, S.J. Rettig, D. Dolphin, Can. J. Chem. 74 (1996) 2182–2193.
- [12] S. ichi Tamaru, L. Yu, W.J. Youngblood, K. Muthukumar, M. Taniguchi, J.S. Lindsey, J. Org. Chem. 69 (2004) 765–777.
- [13] A. Thompson, S.J. Rettig, D. Dolphin, Chem. Commun. (1999) 631–632.
- [14] S.R. Halper, S.M. Cohen, Angew Int. Ed. 43 (2004) 2385–2389.
- [15] B. Moulton, M.J. Zaworotko, Chem. Rev. 101 (2001) 1629–1658.
- [16] S.R. Halper, S.M. Cohen, Inorg. Chem. 44 (2005) 4139–4141.
- [17] S.R. Halper, M.R. Malachowski, H.M. Delancy, S.M. Cohen, Inorg. Chem. 43 (2004) 1242–1245.
- [18] L. Do, S.R. Halper, S.M. Cohen, Chem. Commun. (2004) 2662–2663.
- [19] S.R. Halper, S.M. Cohen, Angew Int. Ed. 43 (2004) 2385–2388.
- [20] V.S. Thoi, J.R. Stork, D. Magde, S.M. Cohen, Inorg. Chem. 45 (2005) 10688–10697.
- [21] S.R. Halper, L. Do, J.R. Stork, S.M. Cohen, J. Am. Chem. Soc. 128 (2006) 15255–15258.
- [22] E.A. Katayev, N.V. Boev, V.N. Khrustalev, Y.A. Ustynyuk, Tananaev, J.L. Sessler, J. Org. Chem. 72 (2007) 2886–2896.
- [23] S. Goeb, R. Ziesel, Tetrahedron Lett. 49 (2008) 2569–2574.
- [24] A. Haeefele, G. Ulrich, P. Retailleau, R. Ziesel, Tetrahedron Lett. 49 (2008) 3716–3721.
- [25] K. Kim, C. Jo, S. Easwaramoorthi, J. Sung, D.H. Kim, D.G. Churchill, Inorg. Chem. 49 (2010) 4881–4894.
- [26] Y. Gu, T. Kar, S. Scheiner, J. Am. Chem. Soc. 121 (1999) 9411–9422.
- [27] F.H. Allen, V.J. Hoy, J.A.K. Howard, V.R. Thalladi, G.R. Desiraju, C.C. Wilson, G.J. McIntyre, J. Am. Chem. Soc. 119 (1997) 3477–3480.
- [28] D. Philp, J.M.A. Robinson, J. Chem. Soc. Perkin Trans. 2 (1998) 1643–1650.
- [29] H. Fischer, H. Hofelmann, Justus Liebig's, Ann. Chem. 533 (1938) 216.
- [30] R.B. Woodward, Angew Chem. 72 (1960) 651.
- [31] R.A. Jones, G.P. Bean, The Chemistry of Pyrroles, Academic Press, London, 1977, 525–528.
- [32] S.J. Hong, M.H. Lee, C.H. Lee, Bull. Korean Chem. Soc. 25 (2004) 1545–1550.
- [33] R.T. Hayes, M.R. Wasilewski, D. Gosztoła, J. Am. Chem. Soc. 122 (2000) 5563–5567.
- [34] M. Harmjan, H.S. Gill, M.J. Scott, J. Am. Chem. Soc. 122 (2000) 10476–10477.
- [35] A. Sour, M.L. Boillot, E. Riviere, P. Lesot, Eur. J. Inorg. Chem. 1999 (1999) 2117–2119.

- [36] R.G. Parr, W. Yang, *Density functional Theory of Atoms and Molecules*, Oxford University Press, Oxford, New York, 1989.
- [37] R.G. Pearson, *J. Org. Chem.* 54 (1989) 1430–1432.
- [38] R.G. Parr, R.G. Pearson, *J. Am. Chem. Soc.* 105 (1983) 7512–7516.
- [39] P. Geerlings, F.D. Proft, W. Langenaeker, *Chem. Rev.* 103 (2003) 1793–1874.
- [40] R.G. Parr, L. Szentpály, S. Liu, *J. Am. Chem. Soc.* 121 (1999) 1922–1924.
- [41] P.K. Chattaraj, U. Sarkar, D.R. Roy, *Chem. Rev.* 106 (2006) 2065–2091.
- [42] M.J. Frisch, G.W. Trucks, H.B. Schlegel, G.E. Scuseria, M.A. Robb, J.R. Cheeseman, J.A. Montgomery Jr., T. Vreven, K.N. Kudin, J.C. Burant, J.M. Millam, S.S. Iyengar, J. Tomasi, V. Barone, B. Mennucci, M. Cossi, G. Scalmani, N. Rega, G.A. Petersson, H. Nakatsuji, M. Hada, M. Ehara, K. Toyota, R. Fukuda, J. Hasegawa, M. Ishida, T. Nakajima, Y. Honda, O. Kitao, H. Nakai, M. Klene, X. Li, J.E. Knox, H.P. Hratchian, J. B. Cross, V. Bakken, C. Adamo, J. Jaramillo, R. Gomperts, R.E. Stratmann, O. Yazyev, A.J. Austin, R. Cammi, C. Pomelli, J.W. Ochterski, P.Y. Ayala, K. Voth, G.A. Morokuma, P. Salvador, J.J. Dannenberg, V.G. Zakrzewski, S. Dapprich, A.D. Daniels, M.C. Strain, O. Farkas, D.K. Malick, A.D. Rabuck, K. Raghavachari, J.B. Foresman, J.V. Ortiz, Q. Cui, A.G. Baboul, S. Clifford, J. Cioslowski, B.B. Stefanov, G. Liu, A. Liashenko, P. Piskorz, I. Komaromi, R.L. Martin, D.J. Fox, T. Keith, M.A. Al-Laham, C.Y. Peng, A. Nanayakkara, M. Challacombe, P.M.W. Gill, B. Johnson, W. Chen, M.W. Wong, C. Gonzalez, and J.A. Pople, *Gaussian 03, Revision C.02*, Gaussian, Inc., Wallingford, CT, 2004.
- [43] A.D. Becke, *J. Chem. Phys.* 98 (1993) 5648–5652.
- [44] C.T. Lee, W.T. Yang, R.G.B. Parr, *Phys. Rev.* 37 (1988) 785–789.
- [45] D.A. Petersson, M.A. Allaham, *J. Chem. Phys.* 94 (1991) 6081–6090.
- [46] R.F.W. Bader, J.R. Cheeseman, In *AIMPAC Ed.*, (2000).
- [47] G.K. Patra, Y.D. Posner, I. Goldberg, *Acta Cryst.* E58 (2002) o530–o531.
- [48] N. Maiti, J. Lee, D.G. Churchill, Y. Do, H.S. Shin, *J. Chem. Crystallogr.* 35 (2005) 949–955.
- [49] K. Wolinski, J.F. Hinton, J.F. Pulay, *J. Am. Chem. Soc.* 112 (1990) 8251–8260.
- [50] I.M. Snehaltha, C. Ravikumar, I. Joe Hubert, N. Sekar, V.S. Jayakumar, *Spectrochim. Acta Part A* 72 (2009) 654–662.
- [51] A.E. Reed, L.A. Curtiss, F. Weinhold, *Chem. Rev.* 88 (1988) 899–926.
- [52] C.G. Liu, Z.M. Su, X.H. Guan, S. Muhammad, *J. Phys. Chem. C* 115 (2011) 23946–23954.
- [53] F. Weinhold, C.R. Landis, *Valency and Bonding: A Natural Bond Orbital–Acceptor Perspective*, Cambridge University Press, Cambridge, New York, Melbourn, 2005. 215–274.
- [54] J.A. Pople, H.B. Schlegel, R. Krishnan, D.J. Defrees, J.S. Binkley, M.J. Frisch, R.A. Whiteside, R.F. Hout, W.J. Hehre, *Int. J. Quantum Chem.* 15 (1981) 269–278.
- [55] A.T. Dubis, S.J. Grabowski, D.B. Romanowska, T. Misiaszek, J. Leszczynski, *J. Phys. Chem. A* 106 (2002) 10613–10621.
- [56] B.M. Giuliano, I. Reva, R. Fausto, *J. Phys. Chem. A* 114 (2010) 2506–2517.
- [57] M.R. Anoop, P.S. Binil, S. Suma, M.R. Sundarsanakumar, S. Mary, H.T. Varghese, C.Y. Panicker, *J. Mol. Struct.* 969 (2010) 233–237.
- [58] P. Pulay, G. Fogarasi, F. Pang, J.E. Boggs, *J. Am. Chem. Soc.* 101 (1979) 2550–2560.
- [59] R.M. Silverstein, F.X. Webster, *Spectrometric Identification of Organic Compounds*, sixth ed., John Wiley Sons Inc., New York, 1963.
- [60] U. Koch, P. Popelier, *J. Phys. Chem. A* 99 (1995) 9747–9754.
- [61] I. Rozas, I. Alkorta, J. Elguero, *J. Am. Chem. Soc.* 122 (2000) 11154–11161.
- [62] E. Espinosa, E. Molins, C. Lecomte, *Chem. Phys. Lett.* 285 (1998) 170–173.
- [63] J. Padmanabhan, R. Parthasarathi, V. Subramanian, P.K. Chattaraj, *J. Phys. Chem. A* 111 (2007) 1358–1361.